

e-ViL: A Dataset and Benchmark for Natural Language Explanations in Vision-Language Tasks

Maxime Kayser^{1*} Oana-Maria Camburu¹ Leonard Salewski² Cornelius Emde¹
 Virginie Do^{1**} Zeynep Akata^{2,3,4} Thomas Lukasiewicz¹

¹Department of Computer Science, University of Oxford ²University of Tübingen

³Max Planck Institute for Intelligent Systems ⁴Max Planck Institute for Informatics

Abstract

Recently, there has been an increasing number of efforts to introduce models capable of generating natural language explanations (NLEs) for their predictions on vision-language (VL) tasks. Such models are appealing, because they can provide human-friendly and comprehensive explanations. However, there is a lack of comparison between existing methods, which is due to a lack of re-usable evaluation frameworks and a scarcity of datasets. In this work, we introduce e-ViL and e-SNLI-VE. **e-ViL is a benchmark for explainable vision-language tasks that establishes a unified evaluation framework and provides the first comprehensive comparison of existing approaches that generate NLEs for VL tasks. It spans four models and three datasets and both automatic metrics and human evaluation are used to assess model-generated explanations. e-SNLI-VE is currently the largest existing VL dataset with NLEs (over 430k instances). We also propose a new model that combines UNITER [15], which learns joint embeddings of images and text, and GPT-2 [38], a pre-trained language model that is well-suited for text generation. It surpasses the previous state of the art by a large margin across all datasets. Code and data are available here: <https://github.com/maximek3/e-ViL>.**

1. Introduction

Deep learning models achieve promising performance across a variety of tasks but are typically black box in nature. There are several arguments for making these models more explainable. For example, explanations are crucial in establishing trust and accountability, which is especially relevant in safety-critical applications such as healthcare or autonomous vehicles. They can also enable us to better understand and correct the learned biases of models [5].

Explainability efforts in vision tasks largely focus on highlighting relevant regions in the image, which can be achieved via tools such as saliency maps [1] or attention maps [47]. Our work focuses on natural language explanations (NLEs), which aim to explain the decision-making process of a model via generated sentences. Besides being easy to understand for lay users, NLEs can explain more complex and fine-grained reasoning, which goes beyond highlighting the important image regions. We compare different models that generate NLEs for vision-language (VL) tasks, i.e., tasks where the input consists of visual and textual information, such as visual question-answering (VQA).

NLEs for VL tasks (VL-NLE) is an emerging field, and only few datasets exist. Moreover, existing datasets tend to be relatively small and unchallenging (e.g., VQA-X [37]) or noisy (e.g., VQA-E [29]). Another limitation of the VL-NLE field is that there is currently no unified evaluation framework, i.e., there is no consensus on how to evaluate NLEs. NLEs are difficult to evaluate, as correct explanations can differ both in syntactic form and in semantic meaning. For example, “Because she has a big smile on her face” and “Because her team just scored a goal” can both be correct explanations for the answer “Yes” to the question “Is the girl happy?”, but existing automatic natural language generation (NLG) metrics are poor at capturing this. As such, the gold standard for assessing NLEs is human evaluation. Past work have all used different approaches for human evaluations, and therefore no objective comparison exists.

In this work, we propose **five main contributions** to address the lack of comparison between existing work. (1) We propose e-ViL, the first **benchmark for VL-NLE tasks**. e-ViL spans across three datasets of human-written NLEs, and provides a **unified evaluation framework** that is designed to be re-usable for future works. (2) Using e-ViL, we compare four VL-NLE models. (3) We introduce e-SNLI-VE, a dataset of over 430k instances, the currently largest dataset for VL-NLE. (4) We introduce a **novel model, called e-UG**,

*Corresponding Author: maxime.kayser@cs.ox.ac.uk

**Now at Université Paris-Dauphine, PSL, and Facebook AI Research.

which surpasses the state of the art by a large (and significant) margin across all three datasets. (5) We provide the currently largest study on the correlation between automatic NLG metrics and human evaluation of NLEs.

2. Related Work

Explainability in Computer Vision. Common approaches to explainability of deep learning methods in computer vision are saliency maps [1], attention maps [47], and activation vectors [25]. Saliency and attention maps indicate where a model looks. This may tell us what regions of the image are most important in the decision-making process of a model. Activation vectors are a way to make sense of the inner representation of a model, e.g., by mapping it to human-known concepts. However, these approaches often cover only a fraction of the reasoning of a model. On the contrary, NLEs can convey higher-order reasoning and describe complex concepts. For example, in Figure 1, highlighted image regions or weights for different concepts would not be sufficient to explain the answer. Additionally, it has been shown that numerical or visual explanatory methods, in some cases, can be confusing even for data scientists [24] and can pose problems even for explaining trivial models [13].

NLEs. First adoptions of NLEs have been in image classification [23] and were further extended to self-driving cars [26], VQA [37], and natural language processing [11; 39; 9; 6; 27; 35; 28; 12]. The most important works in VL-NLE [37; 46; 34] are included in this benchmark.

VL-NLE Datasets. Existing models learn to generate NLEs in a supervised manner and, therefore, require training sets of human-written explanations. Besides the image classification datasets ACT-X [37] and CUB [43; 23], and the video dataset BDD-X [26], there are currently three VL datasets with NLEs. The VQA-X dataset [37] was introduced first and provides NLEs for a small subset of questions from VQA v2 [4]. It consists of 33k QA pairs (28k images). However, many of the NLEs in VQA-X are trivial and could be guessed without looking at the image. For example, “because she is riding a wave on a surfboard” is an NLE for the answer “surfing” to the question “What is the woman in the image doing?” that can easily be guessed from the answer, without looking at the image (more examples are given in Figure 6). VQA-E [29] is another dataset that also builds on top of VQA v2. However, its explanations are gathered in an automatic way and were found to be of low quality by Marasović et al. [34], where the model-generated explanations obtain a human evaluation accuracy¹ that is only 3% short of the VQA-E ground-truth explanations (66.5%), suggesting that the dataset is essentially solved. It is therefore not used in our benchmark. Finally, the VCR dataset [50]



Question: What would happen if 3 were to give 4 a bottle of wine?
Answer: 4 would drink the wine until he was drunk.
GT Explanation: 4 is sad and people tend to drink excessively when they are sad and drinking excessively leads to becoming drunk, there for 4 would drink until he was drunk.

Figure 1: VCR images require commonsense reasoning that often goes beyond the visual content of the image.

provides NLEs for VQA instances that require substantial commonsense knowledge (see Figure 1). The questions are challenging, and therefore both the answers and NLEs are given in the form of multiple-choice options.

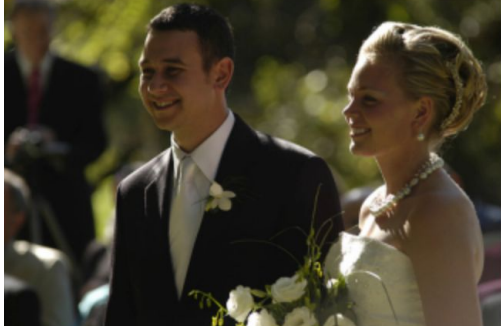
Our proposed dataset, e-SNLI-VE, extends the range of VL-NLE datasets and addresses some of the prior limitations. It contains over 430k instances for which the explanations rely on the image content (see examples in Figure 6). We will describe the dataset in more detail in Section 3.

Evaluations and Comparisons. Evaluating NLG is challenging and a much-studied field [19]. Evaluating NLEs is even more difficult, as sentences may not only differ in their syntactic form but also in their semantic meaning, e.g., there can be several different reasons why a sentence contradicts an image. For this reason, current automatic NLG metrics, such as the BLEU score [36], do not perform well in evaluating NLEs [11]. Hence, several works have used human evaluation to assess their generated explanations [37; 46; 34; 17]. However, they all used different evaluation rules, preventing one from being able to compare existing VL-NLE models. The main differences lie in the datasets used, the questions asked to annotators, whether the assessment is absolute or based on a ranking, and the formula used to calculate the final score. We select the best practices from existing evaluation schemes and develop a unified and re-usable human evaluation framework for VL-NLE.

3. The e-SNLI-VE Dataset

We introduce e-SNLI-VE, a large-scale dataset for visual-textual entailment with NLEs. We built it by merging the explanations from e-SNLI [11] and the image-sentence pairs from SNLI-VE [48]. We use several filters and manual relabeling steps to address the challenges that arise from

¹Percentage of explanations that, given the image and question, support the predicted answer.



Hypothesis: A man and woman inside a church.
Textual premise: A man and woman getting married.
Original label: Neutral
Caption #2: A man and woman that is holding flowers smile in the sunlight.
Caption #4: A happy couple enjoying their open air wedding.

Figure 2: The original label of the textual premise-hypothesis pair in SNLI is neutral. However, by considering alternative captions describing the same image (#2 and #4), we can deduct that the neutral label is false.

merging these datasets. The validation and test sets were relabeled by hand. The dataset is publicly available².

3.1. Correcting SNLI-VE

In SNLI-VE [48], an image and a textual hypothesis are given, and the task is to classify the relation between the image-premise and the textual hypothesis. The possible labels are *entailment* (if the hypothesis is true, given the image), *contradiction* (the hypothesis is false, given the image), or *neutral* (if there is not enough evidence to conclude whether the hypothesis is true or false). SNLI-VE builds off the SNLI [10] dataset, by replacing textual premises with Flickr30k images [49]. This is possible, because the textual premises in SNLI are caption sentences of those images. However, this replacement led to labeling errors, as an image typically contains more information than a single caption describing it. Especially for the neutral class, a caption may not have enough evidence to suggest entailment or contradiction, but the corresponding image does (see Figure 2). On a manually evaluated subset of 535 samples, we found a 38.6% error rate among the neutral labels. This subset will be used below to evaluate the effectiveness of our filters. Error rates for entailment and contradiction are reported to be under 1% [48], hence we focus only on correcting the neutral instances.

In the validation and test sets, we relabeled the neutral examples using Amazon Mechanical Turk (MTurk). To ensure high-quality annotations, we used a series of quality control measures, such as in-browser checks, inserting trusted examples, and collecting three annotations per instance. In total, 39% of the neutral labels were changed to entailment or contradiction. The label distribution shifted from uniform

to Ent/Neut/Cont of 39%/20%/41% and 39%/21%/40% for the validation and test sets, respectively.

For the training set, we propose an automatic way to remove false neutrals. We discovered that the five captions that come with each image often provide clues whether the label is indeed neutral, or not. For every image-hypothesis pair i , we ran a natural language inference model m_{nli} on each caption-hypothesis pair $p_{i,c}$, where c is one of the captions. If the original label of image-hypothesis pair i is neutral, but $\sum_c m_{\text{nli}}(p_{i,c})$ indicates with high confidence that the label is not neutral, we deem the label incorrect and removed the instance from the dataset. An example is shown in Figure 2. For m_{nli} , we used Roberta-large [33] trained on the MNLI dataset [44]. Instances were removed if $\sum_c m_{\text{nli}}(p_{i,c})$ exceeded 2.0 for entailment and contradiction classes. On our 535-samples subset, this filter decreased the error of neutral labels from 39% to 24%. When validated against the relabeling on the validation set, the error decreased from 39% to 30%.

3.2. Adding Explanations to SNLI-VE

To create e-SNLI-VE, we source explanations from e-SNLI [11], which **extends SNLI with human-written NLEs**. However, the explanations in e-SNLI are tailored to the textual premise-hypothesis pairs and are therefore **not always well-suited for the image-hypothesis pair**. After simply merging both datasets, we found that initially 36%, 22%, and 42% of explanations were of low (incorrect), medium (correct, but there is an obvious better choice), and high quality (correct and relevant), respectively. We propose several steps to detect and remove explanations of low and medium quality. The filters were designed to ensure an optimal trade-off between precision and recall (for flagging bad explanations) and with the constraint that the final dataset remains reasonably balanced.

Re-annotation. First, we replace the explanations for the neutral pairs in the validation and test sets with new ones, collected via MTurk at the same time as we collected new labels for these subsets. In order to submit the annotation of an image-sentence pair, workers must choose a label, highlight words in the hypothesis, and use at least half of the highlighted words in the explanation.

Keyword Filter. Next, we use keyword filtering to detect explanations that make reference to a linguistic feature of the textual premise. The keywords, which we manually defined, are “synonym”, “mention”, “rephrasing”, “sentence”, “way to say”, and “another word for”. The keyword filter removed 4.6% of all instances, and our 535-samples subset suggests that *all* filtered explanations were indeed of low quality.

Similarity Filter. We noticed that the share of low-quality explanations is highest for entailment examples. This happens frequently when the textual premise and hypothesis are almost identical, as then the explanation often just repeats

²<https://github.com/maximek3/e-ViL>

	Train	Validation	Test
# Image-Hypothesis pairs (# Images)	401,717 (29,783)	14,339 (1,000)	14,740 (1,000)
Label distribution (C/N/E, %)	36.0 / 31.3 / 32.6	39.4 / 24.0 / 36.6	38.8 / 25.8 / 35.4
Mean hypothesis length (median)	7.4 (7)	7.3 (7)	7.4 (7)
Mean explanation length (median)	12.4 (11)	13.3 (12)	13.3 (12)

Table 1: e-SNLI-VE summary statistics. C, N, and E stand for Contradiction, Neutral, and Entailment, respectively.

both statements. To overcome this, we removed all examples where the ROUGE-1 score (a measure for sentence similarity [31]) between the textual premise and hypothesis was above 0.57. This reduced the share of low-quality explanations for entailment by 4.2%.

Uncertainty Filter. Lastly, we found that image-hypothesis pairs with high uncertainty are correlated with low-quality explanations for contradictions. We define uncertainty as the diversion of the scores from $m_{\text{nli}}(p_{i,c})$ for the five image captions. m_{nli} is the same Roberta-large model that was described above. This filter reduced the share of low-quality explanations for contradiction examples by 5.1%.

The final e-SNLI-VE dataset statistics are displayed in Table 1. An additional evaluation of e-SNLI-VE by external annotators, and a comparison with existing VL-NLE datasets, is provided in Table 2. The results indicate that the quality of the e-SNLI-VE ground-truth explanations is not far off the human-annotated VQA-X and VCR datasets. Qualitative examples and a more detailed rundown of our filtering methods are in Appendix B.

4. The e-ViL Benchmark

In this section, we introduce the VL-NLE task, describe how explanations are evaluated in e-ViL, and describe the datasets covered in our benchmark.

4.1. Task Formulation

We denote a module that solves a VL task as M_T , which takes as input visual information V and textual information L . Its objective is to complete a task T where the outcome is a , i.e., $M_T(V, L) = a$. An example of a VL task is VQA, where V is an image, L is a question, and T is the task of providing the answer a to that question. We extend this by an additional task E , which requires an NLE e justifying how V and L lead to a , solved by the module $M_E(V, L) = e$. The final model M then consists of M_T and M_E . Thus, $M = (M_T, M_E)$ and $M(V, L) = a, e$.

4.2. Datasets

Our benchmark uses the following three datasets, which vary in size and domain. Examples are shown in Figure 6 in the appendix.

e-SNLI-VE. Our proposed e-SNLI-VE dataset has been described in Section 3.

VQA-X. VQA-X [37] contains human written explanations for a subset of questions from the VQA v2 dataset [21]. The image-question pairs are split into train, dev, and test with 29.5k, 1.5k, and 2k instances, respectively. The task *T* is formulated as a multi-label classification task of 3,129 different classes. One question can have multiple possible answers.

VCR. Visual Commonsense Reasoning (VCR) is a VL dataset that asks multiple-choice (single answer) questions about images from movies [50]. In addition to four answer options, it also provides four NLEs options, out of which one is correct. For the purpose of our proposed VL-NLE task, we reformulate it as an explanation generation task. As the test set for VCR is not publicly available, we split the original train set into a train and dev set, and use the original validation set as test set. The splits are of size 191.6k, 21.3k, and 26.5k, respectively.

Human Evaluation of Datasets. In our benchmark experiments (Section 5), human annotators evaluate the ground-truth explanations of all three datasets. For each dataset, 300 examples are evaluated by 12 annotators each, resulting in 3,600 evaluations. The results in Table 2 show that e-SNLI-VE comes close to the manually annotated datasets VCR and VQA-X (82.8% explanations with *yes* or *weak yes* vs. 87.9% and 91.4%). Besides the use of effective, but imperfect, automatic filters, another explanation for the higher share of noise is the trickiness (out of a 100 human re-annotated explanations for neutral examples, we found that 17% had flaws, identical to the share of (weak) no in Table 2) and ambiguity (when three of us chose the labels for a set of 100 image-hypothesis pairs, we only had full agreement on 54% of examples) inherent in the e-SNLI-VE task.

	No	Weak No	Weak Yes	Yes
e-SNLI-VE	10.3%	6.9%	27.7%	55.1%
VQA-X	4.1%	4.5%	25.1%	66.3%
VCR	6.9%	5.2%	36.6%	51.3%

Table 2: Human evaluation of the ground-truth explanations for the three datasets used in e-ViL. The question asked was: “Given the image and the question/hypothesis, does the explanation justify the answer?”.

4.3. Evaluation

Evaluation Scores. We define separate evaluation scores S_T , S_E , and S_O for M_T , M_E , and M , respectively. S_T is the metric that is defined by the original VL task T , e.g., label accuracy for e-SNLI-VE and VCR, and VQA accuracy for VQA-X. We define S_E as the average explanation score of the examples for which the answer a was predicted correctly. In line with previous work [37; 46; 34], we for now assume the simplified scenario that an explanation is always false when it justifies an incorrect answer. The explanation score can be any custom human or automatic metric. Due to the limitations of current automated NLG metrics for evaluating NLEs, we developed a human evaluation framework for computing S_E , outlined in the paragraph below. Finally, we want S_O to summarize the performance of a model on both tasks T and E , to give us the overall performance of a VL-NLE model M . We define $S_O = S_T S_E$, which equates to the average of the scores of all explanations, but where we set the score of an explanation to 0 if its associated answer was predicted incorrectly. This can also be viewed the explanation score S_E multiplied by a coefficient for task performance (accuracy, in most cases). We introduced this measure to avoid giving an advantage to models that purely optimize for generating a few good explanations but neglect the task itself.

Human Evaluation Framework. We collect human annotations on MTurk, where we ask the annotators to proceed in two steps. First, they have to solve the task T , i.e., provide the answer a to the question. This ensures the annotators reflect on the question first and enables us to do in-browser quality checks (since we know the answers). We disregard their annotation if they answered the VL task T incorrectly.

For each explanation, we ask them a simple evaluation question: “Given the image and the question/hypothesis, does the explanation justify the answer?”. We follow Marasović et al. [34] in giving four response choices: *yes*, *weak yes*, *weak no*, and *no*. We map *yes*, *weak yes*, *weak no*, and *no* to the numeric scores of 1, $\frac{2}{3}$, $\frac{1}{3}$, and 0, respectively.

We also ask annotators to select the main shortcomings (if any) of the explanations. We observe three main limitations of explanations. First, they can *insufficiently justify the answer*. For example, the sentence “because it’s cloudy” does not sufficiently justify the answer “the sea is not calm”. Second, an explanation can *incorrectly describe the image*, e.g., if a model learned generic explanations that are not anchored in the image. “There is a person riding a surfboard on a wave” is generally a good explanation for the answer “surfing” when asked “what activity is this?”, but the image may actually display a dog surfing. Lastly, the sentences can be *nonsensical*, such as “a man cannot be a man”.

For each model-dataset pair, we select a random sample of 300 datapoints where the model answered the question correctly. Every sample contains only unique images. For

VCR, all movies are represented in the samples. Note that it is not possible to evaluate all models on exactly the same instances, as they do not all answer the same questions correctly. Taking a subset of examples where *all* models answered correctly is disadvantageous for two reasons. First, this makes the benchmark less re-usable, as future methods might not answer the same questions correctly. Second, this would bias the dataset towards the questions that the weakest model answered correctly. However, in order to still maximize the overlap between the samples, we shuffled all the instances in the test sets randomly and then for each model we took the 300 first on which the answer was correct.

We propose several measures to further ensure robustness and re-usability of the framework. In order to account for annotator subjectivity, we evaluate every instance by three different annotators. The final score per explanation is given by the average of all evaluations. In addition, we evaluate one model at a time to avoid potential anchoring effects between models (e.g., the annotator evaluates one model more favorably, because they are influenced by poor explanations from a different model). To implicitly induce a uniform anchoring effect, the annotators evaluate both the ground-truth explanation (which is invariant to the model) and the explanation generated by a model for every image-question pair. They do not know which is which and are not asked to compare them. This implicitly ensures that all evaluations have the same anchor (the ground-truth) and it allows us to compute S_E in different ways, as outlined in Appendix E.4. Overall, over 200 individual annotators were employed for the benchmark and all of them had to have a 98% prior acceptance rate on MTurk. Finally, we bolster our results with statistical tests in Appendix E.3.

More details and screenshots of our MTurk evaluation can be found in Appendix E. For re-usability, we publicly release the questionnaires used in our benchmark³.

5. Experimental Evaluation

5.1. Models

Existing VL-NLE models follow a common high-level structure (Figure 3). First, a VL model learns a joint representation of the image and language inputs and predicts the answer. The models in this work then condition their explanation on different combinations of the question, image, their joint representation, and the answer. Details on PJ-X [37], FME [46], and RVT [34] are given in Appendix C, as well as in their respective papers.

e-UG. Marasović et al. [34] generate convincing explanations, but out of various M_T modules tested, including complex visual reasoning models, it obtains the best explanation accuracy when using object labels as the sole image information. We address this limitation by proposing e-UG, a model

³<https://github.com/maximek3/e-ViL>

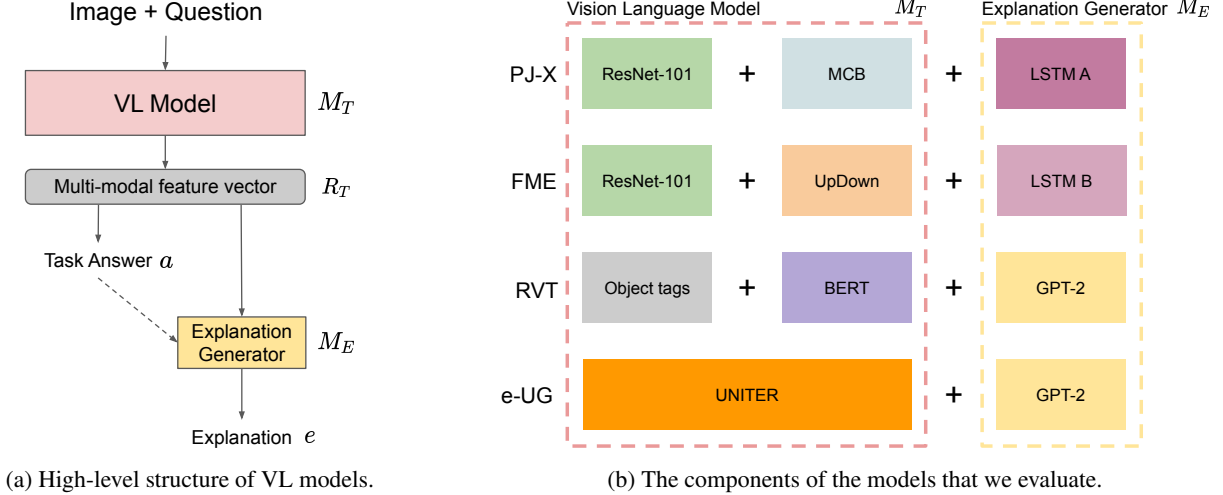


Figure 3: High-level architectures of the models that are included in our benchmark.

that enables a stronger image conditioning by combining GPT-2 with UNITER [15], a powerful transformer-based VL model. The outputs of UNITER are contextualized embeddings of the word tokens and image regions in the image-text pair. Words are embedded by tokenizing them into Word-Pieces and adding their position embedding. Images are embedded by extracting visual features of regions with Faster R-CNN [40] and encoding their location features. UNITER achieves SOTA on many downstream tasks when fine-tuned on them. For e-UG, we leverage these contextualized embeddings to condition GPT-2 on an efficient representation of the image and question. The embeddings of the image regions and question words are simply prepended to the textual question and predicted answer, and then fed to GPT-2. GPT-2 is a decoder-only architecture that is pre-trained on conventional language modeling and therefore well-suited for language generation [38]. We follow Marasović et al. [34] and do greedy decoding during inference.

5.2. Training

All models are trained separately on each dataset. To ensure comparability, image features for PJ-X and FME are obtained from the same ResNet-101 [22] pre-trained on ImageNet, which yields a 2048d feature representation for an image. To account for the small size of VQA-X, the VQA M_T models were pre-trained on VQA v2 for VQA-X, and trained from scratch for the other two datasets. For UNITER, we follow the pre-training procedures used in the original paper [15]. The object tags in RVT are obtained from a Faster R-CNN that was trained on ImageNet and COCO. For GPT-2, we load the pre-trained weights of the original GPT-2 with 117M parameters [38]. For all models in this work, we experimented with training the M_T and M_E modules jointly and separately. More details are given in Appendix C.2.

Hyperparameters. Choosing hyperparameters via human evaluation is prohibitively expensive. Instead, we defined a set of automatic NLG metrics that we used to approximate the selection of the best hyperparameters. We define the score of an explanation as the harmonic mean of the BERTScore F1 [51] and NGRAMScore, where we set NGRAMScore as the harmonic mean of the n -gram NLG metrics ROUGE-L [30], SPICE [2], CIDEr [42], and ME-TEOR [8]. We pick the harmonic mean, as it puts more emphasis on the weaker scores. Further details on the hyperparameters are given in Appendix C.4.

5.3. Results

In this section, we highlight the human evaluation results, their correlation with automatic NLG metrics, and the effect that training with explanations has on the performance on task T . Model performance for automatic NLG metrics, detailed results on e-SNLI-VE, alternative computations of the human evaluation score, and a statistical analysis of the results is provided in Appendix E.

5.3.1 Human Evaluation

The explanation scores S_E obtained from the e-ViL human evaluation framework are displayed in Table 3. Our model e-UG outperforms existing methods on all datasets, with an average S_E score 5.7 points higher than the second-best model, RVT. Despite leveraging little image information, RVT achieves higher scores than PJ-X and FME on average, reflecting the ability of GPT-2 to learn to generate convincing explanations, without much anchoring on the image. There is still a significant gap between S_E scores of generated explanations and ground-truth (GT) explanations. For VQA-X, S_E scores are higher overall, indicating that the dataset is easier. In terms of the overall score S_O , the gap between e-UG and the rest increases further, as UNITER achieves a

	Overall	VQA-X				e-SNLI-VE			VCR		
	S_E	S_O	S_T	S_E	S_O	S_T	S_E	S_O	S_T	S_E	
PJ-X	59.2	49.9	76.4	65.4	41.2	69.2	59.6	20.6	39.0	52.7	
FME	60.1	47.7	75.5	63.2	43.1	73.7	58.5	28.6	48.9	58.5	
RVT	62.8	46.0	68.6	67.1	42.8	72.0	59.4	36.4	59.0	61.8	
e-UG	68.5	57.6	80.5	71.5	54.8	79.5	68.9	45.5	69.8	65.1	
GT	79.3	–	–	84.5	–	–	76.2	–	–	77.3	

Table 3: e-ViL benchmark scores. S_O , S_T , and S_E are defined in Section 4.3. GT denotes the ground-truth explanations in each dataset. The best results are in bold.

higher performance on VL tasks than the M_T modules of the other models. In Figure 4, we show an example with the explanations generated by each model. In this example, e-UG is the only model that accurately describes the image and justifies the answer. Additional examples are given in Figure 5 in the appendix.

As a second question, we ask the annotators to select the shortcomings (if any) for every explanation. Results for this are given in Table 5. The most frequent shortcoming is an insufficient justification of the answer. Least frequent, with around 10% prevalence, explanations can be nonsensical (e.g., “a woman is a woman”). All models struggle similarly much with producing explanations that sufficiently justify the answer. e-UG and PJ-X are better at producing coherent sentences. e-UG is significantly superior in terms of the explanations accurately describing the image content. This empirically confirms the effectiveness of our enhanced conditioning on the image. On a dataset level, we see that it is easiest for all models to provide explanations that make grammatical sense and justify the answer on VQA-X, reinforcing the notion that the explanations of VQA-X are easier and less elaborate.

A statistical analysis of our findings are given in Appendix E.

5.3.2 Correlation of NLG Metrics with Human Evaluation

To better understand to what extent automatic NLG metrics are able to mirror human judgment of explanations, we compute the Spearman correlation of different NLG metrics with the human evaluation scores. The NLG metrics for the different models are given in Appendix E.1. The human evaluation score is averaged and normalised (across all annotators) for each explanation. We have human evaluation scores for a total of 3,566⁴ generated explanations, which makes it the currently largest study on the correlation of NLG metrics with human evaluation in NLEs.

⁴We have 4 models, 3 datasets of 300 examples, therefore 3,600 explanations. However, for 34 of them, all the three annotators answered the question incorrectly.



Hypothesis: The people are flying kites at the beach.
Answer: Contradiction
RVT: People can't be riding kites while they are flying kites.
PJ-X: People cannot be flying and flying at the same time.
FME: People cannot be walking and flying kites at the same time
e-UG: People cannot be flying kites while they are standing on a street.
GT Explanation: construction site is different from the beach

Figure 4: Generated explanations for each model on an image-hypothesis pair in e-SNLI-VE.

The results in Table 6 show that BERTScore and METEOR exhibit significantly higher correlation with human annotators across all datasets, reaching a maximal value of 0.293, which is a relatively low correlation. The reliability of automatic metrics also differs by dataset. They are highest on VQA-X and lowest on VCR. This could be explained by the fact that explanations in VCR are generally semantically more complex or more speculative (and, therefore, there are more different ways to explain the same thing) than those in VQA-X. It is noteworthy that some n -gram metrics, such as BLEU, ROUGE, or CIDEr, have no statistically significant correlation with human judgment on VCR.

5.3.3 Explanations as Learning Instructions

Training a model jointly on the tasks T and E can be viewed as a form of multi-task learning [14]. The explanations e augment the datapoints of task T by explaining why an answer a was given. The module M_T (which solves task T) may bene-

Model	M_T model	VQA-X		SNLI-VE		VCR	
		M_T only	Joint	M_T only	Joint	M_T only	Joint
PJ-X	MCB [18]	N.A.	N.A.	<u>69.7</u>	69.2	38.5	<u>39.0</u>
FME	UpDown [3]	N.A.	N.A.	71.4	<u>73.7</u>	35.7	<u>48.9</u>
e-UG	UNITER [15]	80.0	<u>80.5</u>	79.4	<u>79.5</u>	69.3	<u>69.8</u>

Table 4: Comparison of task scores S_T (e.g., accuracies) when the models are trained only on task T vs. when trained jointly on tasks T and E . Scores are underlined if their difference is greater than 0.5.

Model	Untrue to Image	Lack of Justification	Non-sensical Sentence
PJ-X	25.0%	26.4%	8.9%
RVT	20.4%	24.2%	12.0%
FME	21.8%	23.1%	13.7%
e-UG	15.9%	25.0%	7.4%
Dataset			
e-SNLI-VE	21.3%	28.7%	12.8%
VCR	21.0%	31.2%	11.7%
VQA-X	20.0%	15.4%	7.4%

Table 5: Main shortcomings of the generated explanations, by models and by datasets. Human judges could choose multiple shortcomings per explanation. The best model results are in bold.

Metric	All datasets	VQA-X	e-SNLI-VE	VCR
BLEU-1	0.222	0.396	0.123	<i>0.032</i>
BLEU-2	0.236	0.412	0.142	<i>0.034</i>
BLEU-3	0.224	0.383	0.139	<i>0.039</i>
BLEU-4	0.216	0.373	0.139	<i>0.038</i>
METEOR	0.288	0.438	0.186	0.113
ROUGE-L	0.238	0.399	0.131	<i>0.050</i>
CIDEr	0.245	0.404	0.133	<i>0.093</i>
SPICE	0.235	0.407	0.162	0.116
BERTScore	0.293	0.431	0.189	0.138
BLEURT [41]	0.248	0.338	0.208	0.128

Table 6: Correlation between human evaluation and automatic NLG metrics on NLEs. All values, except those in *italic*, have p-values < 0.001 .

fit from this additional signal. Indeed, the model is forced to learn a representation of the image and question from which both the answer and explanation can be extracted, which could improve the model’s representation capabilities. To verify this hypothesis, we compare the task scores of modules M_T that trained only on task T and those that, together with M_E , were jointly trained on tasks T and E . We do this for e-UG on all three datasets, and for FME and PJ-X on VCR and e-SNLI-VE (because a larger pre-training dataset exists for VQA-X). The results in Table 4 show that, without

any adaptations, the task performance for joint training is equal or better in all but one model-dataset combination. These results suggests that explanations may have the potential to act as “learning instructions” and thereby improve the classification capabilities of a model. Additional experiments are required to further verify this and to develop approaches that more efficiently leverage the explanations.

6. Summary and Outlook

We addressed the lack of comparison between existing VL-NLE methods by introducing **e-ViL**, a unified and reusable benchmark on which we evaluated four different architectures using human judges. We also introduced e-SNLI-VE, the largest existing VL dataset with human-written explanations. The e-ViL benchmark can be used by future works to compare their VL-NLE models against existing ones. Furthermore, our correlation study has shown that automatic NLG metrics have a weak correlation with human judgment. In this work, we also **propose a new model, e-UG**, which leverages contextualized embeddings of the image-question pairs and achieves a state-of-the-art performance by a large margin on all datasets.

Important questions that need to be addressed in future work are the faithfulness of the explanations (i.e., that they faithfully reflect the model reasoning) and the development of automatic NLG metrics that have a stronger correlation with human judgment.

Acknowledgements

Maxime Kayser, Leonard Salewski, and Cornelius Emde are supported by Elsevier BV, the International Max Planck Research School for Intelligent Systems, and by Cancer Research UK (grant number C2195/A25014), respectively. This work has been partially funded by the ERC (853489—DEXIM) and by the DFG (2064/1—Project number 390727645). This work has also been supported by the Alan Turing Institute under the EPSRC grant EP/N510129/1, by the AXA Research Fund, the ESRC grant “Unlocking the Potential of AI for English Law”, the EPSRC grant EP/R013667/1, and by the EU TAILOR grant. We also acknowledge the use of Oxford’s Advanced Research Computing (ARC) facility, of the EPSRC-funded Tier 2 facility JADE (EP/P020275/1), and of GPU computing support by Scan Computers International Ltd.

References

- [1] Marco Ancona, Enea Ceolini, Cengiz Öztireli, and Markus Gross. Towards better understanding of gradient-based attribution methods for deep neural networks. In *6th International Conference on Learning Representations, ICLR 2018, Vancouver, BC, Canada, April 30 - May 3, 2018, Conference Track Proceedings*, 2018.
- [2] Peter Anderson, Basura Fernando, Mark Johnson, and Stephen Gould. SPICE: Semantic propositional image caption evaluation. In *Proceedings of the European Conference on Computer Vision*. Springer, 2016.
- [3] Peter Anderson, Xiaodong He, Chris Buehler, Damien Teney, Mark Johnson, Stephen Gould, and Lei Zhang. Bottom-up and top-down attention for image captioning and visual question answering. In *Proceedings of the IEEE Conference on Computer Vision and Pattern Recognition*, 2018.
- [4] Stanislaw Antol, Aishwarya Agrawal, Jiasen Lu, Margaret Mitchell, Dhruv Batra, C. Lawrence Zitnick, and Devi Parikh. VQA: Visual Question Answering. In *Proceedings of the International Conference on Computer Vision (ICCV)*, 2015.
- [5] Alejandro Barredo Arrieta, Natalia Díaz-Rodríguez, Javier Del Ser, Adrien Bannetot, Siham Tabik, Alberto Barbado, Salvador García, Sergio Gil-López, Daniel Molina, Richard Benjamins, et al. Explainable artificial intelligence (XAI): Concepts, taxonomies, opportunities and challenges toward responsible ai. *Information Fusion*, 58, 2020.
- [6] Pepa Atanasova, Jakob Grue Simonsen, Christina Lioma, and Isabelle Augenstein. Generating fact checking explanations. In *Proceedings of the 58th Annual Meeting of the Association for Computational Linguistics*, Online, July 2020. Association for Computational Linguistics.
- [7] Jimmy Lei Ba, Jamie Ryan Kiros, and Geoffrey E Hinton. Layer normalization. *arXiv preprint arXiv:1607.06450*, 2016.
- [8] Satantjeet Banerjee and Alon Lavie. Meteor: An automatic metric for mt evaluation with improved correlation with human judgments. In *Proceedings of the ACL Workshop on Intrinsic and Extrinsic Evaluation Measures for Machine Translation and/or Summarization*, 2005.
- [9] Chandra Bhagavatula, Ronan Le Bras, Chaitanya Malaviya, Keisuke Sakaguchi, Ari Holtzman, Hannah Rashkin, Doug Downey, Wen tau Yih, and Yejin Choi. Abductive common-sense reasoning. In *International Conference on Learning Representations*, 2020.
- [10] Samuel R. Bowman, Gabor Angeli, Christopher Potts, and Christopher D. Manning. A large annotated corpus for learning natural language inference. In *Proceedings of the 2015 Conference on Empirical Methods in Natural Language Processing (EMNLP)*, 2015.
- [11] Oana-Maria Camburu, Tim Rocktäschel, Thomas Lukasiewicz, and Phil Blunsom. e-SNLI: Natural language inference with natural language explanations. In *Advances in Neural Information Processing Systems (NeurIPS)*, 2018.
- [12] Oana-Maria Camburu, Brendan Shillingford, Pasquale Minervini, Thomas Lukasiewicz, and Phil Blunsom. Make up your mind! Adversarial generation of inconsistent natural language explanations. In *Proceedings of the Annual Meeting of the Association for Computational Linguistics (ACL)*, July 2020.
- [13] Oana-Maria Camburu, Eleonora Giunchiglia, Jakob Foerster, Thomas Lukasiewicz, and Phil Blunsom. The struggles of feature-based explanations: Shapley values vs. minimal sufficient subsets. In *AAAI Workshop on Explainable Agency in Artificial Intelligence*, 2021.
- [14] Rich Caruana. Multitask learning. *Machine Learning*, 28(1), 1997.
- [15] Yen-Chun Chen, Linjie Li, Licheng Yu, Ahmed El Kholy, Faisal Ahmed, Zhe Gan, Yu Cheng, and Jingjing Liu. Uniter: Universal image-text representation learning. In *Proceedings of the European Conference on Computer Vision*. Springer, 2020.
- [16] Jacob Devlin, Ming-Wei Chang, Kenton Lee, and Kristina Toutanova. Bert: Pre-training of deep bidirectional transformers for language understanding. In *Proceedings of the 2019 Conference of the North American Chapter of the Association for Computational Linguistics: Human Language Technologies, Volume 1 (Long and Short Papers)*, 2019.
- [17] Radhika Dua, Sai Srinivas Kancheti, and Vineeth N. Balasubramanian. Beyond VQA: Generating multi-word answer and rationale to visual questions. *arXiv:2010.12852*, October 2020.
- [18] Akira Fukui, Dong Huk Park, Daylen Yang, Anna Rohrbach, Trevor Darrell, and Marcus Rohrbach. Multimodal compact bilinear pooling for visual question answering and visual grounding. In *Proceedings of the 2016 Conference on Empirical Methods in Natural Language Processing (EMNLP)*, 2016.
- [19] Albert Gatt and Emiel Krahmer. Survey of the state of the art in natural language generation: Core tasks, applications and evaluation. *Journal of Artificial Intelligence Research*, 61, 2018.
- [20] Timnit Gebru, Jamie Morgenstern, Briana Vecchione, Jennifer Wortman Vaughan, Hanna Wallach, Hal Daumé III, and Kate Crawford. Datasheets for datasets. *arXiv preprint arXiv:1803.09010*, 2018.
- [21] Yash Goyal, Tejas Khot, Douglas Summers-Stay, Dhruv Batra, and Devi Parikh. Making the V in VQA matter: Elevating the role of image understanding in visual question answering. In *Proceedings of the IEEE Conference on Computer Vision and Pattern Recognition*, 2017.

- [22] Kaiming He, Xiangyu Zhang, Shaoqing Ren, and Jian Sun. Deep residual learning for image recognition. In *Proceedings of the IEEE Conference on Computer Vision and Pattern Recognition*, 2016.
- [23] Lisa Anne Hendricks, Zeynep Akata, Marcus Rohrbach, Jeff Donahue, Bernt Schiele, and Trevor Darrell. Generating visual explanations. In *Proceedings of the European Conference on Computer Vision*. Springer, 2016.
- [24] Harmanpreet Kaur, Harsha Nori, Samuel Jenkins, Rich Caruana, Hanna Wallach, and Jennifer Wortman Vaughan. Interpreting interpretability: Understanding data scientists’ use of interpretability tools for machine learning. In *Proceedings of the 2020 CHI Conference on Human Factors in Computing Systems*, 2020.
- [25] Been Kim, Martin Wattenberg, Justin Gilmer, Carrie Cai, James Wexler, Fernanda Viegas, et al. Interpretability beyond feature attribution: Quantitative testing with concept activation vectors (TCAV). In *Proceedings of the International Conference on Machine Learning (ICML)*, 2018.
- [26] Jinkyu Kim, Anna Rohrbach, Trevor Darrell, John Canny, and Zeynep Akata. Textual explanations for self-driving vehicles. In *Proceedings of the European Conference on Computer Vision (ECCV)*, 2018.
- [27] Neema Kotonya and Francesca Toni. Explainable automated fact-checking for public health claims. In *Proceedings of the 2020 Conference on Empirical Methods in Natural Language Processing (EMNLP)*, Online, November 2020. Association for Computational Linguistics.
- [28] Sawan Kumar and Partha Talukdar. NILE: Natural language inference with faithful natural language explanations. In *Proceedings of the 58th Annual Meeting of the Association for Computational Linguistics*, pages 8730–8742, Online, July 2020. Association for Computational Linguistics.
- [29] Qing Li, Qingyi Tao, Shafiq Joty, Jianfei Cai, and Jiebo Luo. VQA-E: Explaining, elaborating, and enhancing your answers for visual questions. In *Proceedings of the European Conference on Computer Vision (ECCV)*, 2018.
- [30] Chin-Yew Lin and Franz Josef Och. Automatic evaluation of machine translation quality using longest common subsequence and skip-bigram statistics. In *Proceedings of the 42nd Annual Meeting of the Association for Computational Linguistics (ACL-04)*, 2004.
- [31] CY LIN. Rouge: A package for automatic evaluation of summaries. In *Text Summarization Branches Out: Proceedings of the ACL-04 Workshop, Barcelona, Spain*, pages 74–81, 2004.
- [32] Shikun Liu, Edward Johns, and Andrew J Davison. End-to-end multi-task learning with attention. In *Proceedings of the IEEE/CVF Conference on Computer Vision and Pattern Recognition*, 2019.
- [33] Yinhan Liu, Myle Ott, Naman Goyal, Jingfei Du, Mandar Joshi, Danqi Chen, Omer Levy, Mike Lewis, Luke Zettlemoyer, and Veselin Stoyanov. RoBERTa: A robustly optimized BERT pretraining approach. *arXiv preprint arXiv:1907.11692*, 2019.
- [34] Ana Marasović, Chandra Bhagavatula, Jae sung Park, Ronan Le Bras, Noah A Smith, and Yejin Choi. Natural language rationales with full-stack visual reasoning: From pixels to semantic frames to commonsense graphs. In *Proceedings of the 2020 Conference on Empirical Methods in Natural Language Processing: Findings*, 2020.
- [35] Sharan Narang, Colin Raffel, Katherine Lee, Adam Roberts, Noah Fiedel, and Karishma Malkan. WT5?! Training Text-to-Text Models to Explain their Predictions. *arXiv:2004.14546 [cs]*, April 2020.
- [36] Kishore Papineni, Salim Roukos, Todd Ward, and Wei-Jing Zhu. BLEU: A method for automatic evaluation of machine translation. In *Proceedings of the 40th Annual Meeting of the Association for Computational Linguistics*, 2002.
- [37] Dong Huk Park, Lisa Anne Hendricks, Zeynep Akata, Anna Rohrbach, Bernt Schiele, Trevor Darrell, and Marcus Rohrbach. Multimodal explanations: Justifying decisions and pointing to the evidence. In *Proceedings of the IEEE Conference on Computer Vision and Pattern Recognition*, 2018.
- [38] Alec Radford, Jeffrey Wu, Rewon Child, David Luan, Dario Amodei, and Ilya Sutskever. Language models are unsupervised multitask learners. *OpenAI blog*, 1(8), 2019.
- [39] Nazneen Fatema Rajani, Bryan McCann, Caiming Xiong, and Richard Socher. Explain yourself! Leveraging language models for commonsense reasoning. In *Proceedings of the Annual Meeting of the Association for Computational Linguistics (ACL)*, 2019.
- [40] Shaoqing Ren, Kaiming He, Ross B Girshick, and Jian Sun. Faster r-cnn: Towards real-time object detection with region proposal networks. In *Proceedings of the Conference on Neural Information Processing Systems (NeurIPS)*, 2015.
- [41] Thibault Sellam, Dipanjan Das, and Ankur Parikh. Bleurt: Learning robust metrics for text generation. In *Proceedings of the 58th Annual Meeting of the Association for Computational Linguistics*, 2020.
- [42] Ramakrishna Vedantam, C. Lawrence Zitnick, and Devi Parikh. CIDEr: Consensus-based image description evaluation. In *Proceedings of the IEEE Conference on Computer Vision and Pattern Recognition*, 2015.
- [43] P. Welinder, S. Branson, T. Mita, C. Wah, F. Schroff, S. Belongie, and P. Perona. Caltech-UCSD Birds 200. Technical Report CNS-TR-2010-001, California Institute of Technology, 2010.
- [44] Adina Williams, Nikita Nangia, and Samuel Bowman. A broad-coverage challenge corpus for sentence understanding

through inference. In *Proceedings of the 2018 Conference of the North American Chapter of the Association for Computational Linguistics: Human Language Technologies, Volume 1 (Long Papers)*, 2018.

- [45] Thomas Wolf, Lysandre Debut, Victor Sanh, Julien Chaumond, Clement Delangue, Anthony Moi, Pierric Cistac, Tim Rault, Rémi Louf, Morgan Funtowicz, Joe Davison, Sam Shleifer, Patrick von Platen, Clara Ma, Yacine Jernite, Julien Plu, Canwen Xu, Teven Le Scao, Sylvain Gugger, Mariama Drame, Quentin Lhoest, and Alexander M. Rush. Transformers: State-of-the-art natural language processing. In *Proceedings of the 2020 Conference on Empirical Methods in Natural Language Processing: System Demonstrations*, Online, October 2020. Association for Computational Linguistics.
- [46] Jialin Wu and Raymond Mooney. Faithful multimodal explanation for visual question answering. In *Proceedings of the 2019 ACL Workshop BlackboxNLP: Analyzing and Interpreting Neural Networks for NLP*, 2019.
- [47] Tianjun Xiao, Yichong Xu, Kuiyuan Yang, Jiaying Zhang, Yuxin Peng, and Zheng Zhang. The application of two-level attention models in deep convolutional neural network for fine-grained image classification. In *Proceedings of the IEEE Conference on Computer Vision and Pattern Recognition*, 2015.
- [48] Ning Xie, Farley Lai, Derek Doran, and Asim Kadav. Visual entailment: A novel task for fine-grained image understanding. *arXiv preprint arXiv:1901.06706*, January 2019.
- [49] Peter Young, Alice Lai, Micah Hodosh, and Julia Hockenmaier. From image descriptions to visual denotations: New similarity metrics for semantic inference over event descriptions. *Transactions of the Association for Computational Linguistics*, 2, 2014.
- [50] Rowan Zellers, Yonatan Bisk, Ali Farhadi, and Yejin Choi. From recognition to cognition: Visual commonsense reasoning. In *Proceedings of the IEEE/CVF Conference on Computer Vision and Pattern Recognition*, 2019.
- [51] Tianyi Zhang, Varsha Kishore, Felix Wu, Kilian Q. Weinberger, and Yoav Artzi. BERTscore: Evaluating text generation with BERT. In *Proceedings of the International Conference on Learning Representations*, 2020.

Appendices

A. Qualitative Examples

Two sets of figures are given to show qualitative examples of our datasets and models. Figure 5 shows the explanations generated by the models (and the ground-truth) for two images of each dataset. We also display the e-ViL S_E score of each generated explanation, which was obtained through our human evaluation framework. In some of the images, such as in Figures 5b and 5f, we can see that e-UG provides better, more image-grounded explanations.

In Figure 6 we again show two images per dataset. These examples illustrate the key differences between the different datasets. VCR has many questions that require substantial commonsense reasoning and general knowledge. For example, to explain the answer to the question in Figure 6e, one needs to know that person 1 is wearing a T-shirt of the classic rock band Guns N’ Roses. For VQA-X (Figures 6c and 6d), we show two examples where a generic explanation, that is not necessarily grounded in the image, will often suffice (this is a general limitation of this dataset). The explanation “Because there is a person on a surfboard” and “Because there is a bed in the room” will, in most cases, be correct with respect to the question and answer, regardless of the image. The examples for e-SNLI-VE in Figures 6a and 6b both require the explanations to describe image-specific characteristics in order to be meaningful. In Figure 6a, a valid explanation would have to pick out a concrete element from the image to explain why it is a contradiction.

B. e-SNLI-VE

This section contains a datasheet on e-SNLI-VE, as well as further information on its pre-processing. Details on the filters are given in Section B.4. Details on the MTurk evaluation can be found in Appendix D.

B.1. e-SNLI-VE Datasheet

The questions in this section will be answered predominantly with respect to the changes that were applied on top of (e-)SNLI, SNLI-VE, and Flickr30k. We use the datasheet form from Gebru et al. [20].

B.1.1 Motivation

For what purpose was the dataset created? The dataset was created for the purpose of extending the range of existing VL-NLE datasets with a large-scale dataset that requires fine-grained reasoning.

Who created the dataset (e.g., which team, research group) and on behalf of which entity (e.g., company, institution, organization)? The dataset was created by researchers from the University of Oxford. It builds on existing

datasets which involved other institutions (NEC Laboratories America for SNLI-VE) and universities (Stanford University for SNLI, University of Illinois at Urbana-Champaign for Flickr30k, University of Oxford for e-SNLI).

B.1.2 Composition

What do the instances that comprise the dataset represent (e.g., documents, photos, people, countries)? Photos (some with people) and natural language sentences.

How many instances are there in total? In total, there are 430,796 instances.

Does the dataset contain all possible instances or is it a sample (not necessarily random) of instances from a larger set? The dataset contains a reduced sample of the original 570k sentence pairs from SNLI [10]. It has been reduced because various filtering methods were applied to remove noise that occurred from combining e-SNLI and SNLI-VE. The filtering steps disproportionately affect the “neutral” class.

What data does each instance consist of? Each instance consists of an image, a natural language hypothesis, a label that classifies the image-hypothesis pair as entailment, contradiction, or neutral, and a natural language explanation that explains why the label was given.

Is any information missing from individual instances? No, all instances contain the complete the information described above.

Are relationships between individual instances made explicit? Yes. Some instances refer to the same image, which is indicated via their image ID.

Are there recommended data splits? Yes, the train, dev, and test splits are given with the release of the dataset.

Are there any errors, sources of noise, or redundancies in the dataset? The labels and explanations were originally annotated for textual premise-hypothesis pairs. By replacing the textual premise with an image, noise occurs. Despite our best efforts to filter out this noise, a considerable error rate remains.

Is the dataset self-contained, or does it link to or otherwise rely on external resources? The dataset needs to be linked with Flickr30k images, which are publicly available.

Does the dataset contain data that might be considered confidential (e.g., data that is protected by legal privilege or by doctor-patient confidentiality, data that includes the content of individuals’ non-public communications)? No.



Hypothesis: A dog is playing with a cat.
Relation: Contradiction
GT Explanation: A man running and a dog playing with a cat are two very distinct activities.
PJ-X: a dog is not a cat
FME: a dog is not a cat
RVT: A cat is not a dog.
e-UG: A dog is not a football player.

Human Evaluation:
 0.00
 0.17
 0.00
 0.56

(a) e-SNLI-VE.



Hypothesis: The lady is the owner of the store.
Relation: Neutral
GT Explanation: We cannot tell from this picture if the lady is the owner of the store.
PJ-X: a woman looking at a microscope does not imply that she is looking for the store
FME: a woman can be a man or a woman
RVT: Just because a lady is holding a book does not mean she is the owner of the store.
e-UG: Just because a lady is working at a store does not mean she is the owner.

Human Evaluation:
 0.56
 0.17
 0.67
 1

(b) e-SNLI-VE.



Question: What sport are they playing?
Answer: tennis
GT Explanation: they are holding tennis rackets inside the court.
PJ-X: the man is holding a tennis racket
FME: they are holding tennis rackets
RVT: the man is holding a racket
e-UG: they are holding tennis rackets

Human Evaluation:
 1
 0.89
 0.89
 1

(c) VQA-X.



Question: What game is the guy playing?
Answer: frisbee
GT Explanation: he is about to catch one in his hand.
PJ-X: he is holding a frisbee
FME: the man is holding a frisbee
RVT: he is holding a disc
e-UG: he is throwing a frisbee.

Human Evaluation:
 0.22
 0.22
 0.33
 0.67

(d) VQA-X.



Question: What is 1 doing ?
Answer: 1 is confronting 3.
GT Explanation: 3 looks uncomfortable and 1 looks as if he is not happy.
PJ-X: 1 is looking at 3 with a smile on his face
FME: 1 is looking at 3 with a frown
RVT: 1 is looking at 3 with a look of anger on his face.
e-UG: 1 is facing 3 and is speaking to him.

Human Evaluation:
 0.00
 0.78
 0.5
 0.89

(e) VCR.



Question: What is in wineglass ?
Answer: There 's champagne in wineglass.
GT Explanation: There 's a bottle of champagne near it.
PJ-X: there is a plate of food in front of her and she is holding a fork
FME: wineglass is a wine glass and wineglass is a wine glass
RVT: wineglass is a wineglass and wineglass is a wineglass.
e-UG: The glass is full of champagne and there is a champagne bottle in front of it.

Human Evaluation:
 0.33
 0.44
 0.67
 1

(f) VCR.

Figure 5: Pair of examples from the test set of each dataset. We display the ground-truth (GT) explanation, as well as the generated explanations of each model and their predicted human evaluation score S_E .



Hypothesis: The man rode his bike.

Relation: Contradiction

(a) e-SNLI-VE.



Hypothesis: A male has a hat on.

Relation: Entailment

(b) e-SNLI-VE.



Question: What sport is this person doing?

Answer: surfing

(c) VQA-X.



Question: What room is this?

Answer: bedroom

(d) VQA-X.



Question: What kind of music does 1 like?

Answer: He likes classic rock.

(e) VCR.



Question: What is 2 doing?

Answer: 2 is communicating with someone outside of the room to give them instruction.

(f) VCR.

Figure 6: Representative examples from each dataset.

B.1.3 Collection Process

How was the data associated with each instance acquired? Hypotheses and explanations were annotated by people. SNLI-VE combined e-SNLI and Flickr30k by replacing the textual premise by an image. This was possible because the textual premises in SNLI are all captions of Flickr30k images. e-SNLI-VE was obtained by associating the explanations from SNLI with SNLI-VE. We used MTurk to reannotate the labels and explanations for the neutral class in the validation and test set. Numerous validation steps have been used to measure the effectiveness of merging, re-annotating, and filtering the dataset.

What mechanisms or procedures were used to collect the data (e.g., hardware apparatus or sensor, manual human curation, software program, software API)? Software program and manual human curation.

B.1.4 Preprocessing/Cleaning/Labeling

Was any preprocessing/cleaning/labeling of the data done (e.g., discretization or bucketing, tokenization, part-of-speech tagging, SIFT feature extraction, removal of instances, processing of missing values)? Various filters were used to remove noise. We used a false neutral detector (details in Section 3.1), a keyword filter (details in Section 3.2), a similarity filter (details in Section 3.2), and an uncertainty filter (details in Section 3.2). We also reannotated all neutral examples in the validation and test set.

B.1.5 Distribution

Will the dataset be distributed to third parties outside of the entity (e.g., company, institution, organization) on behalf of which the dataset was created? The dataset is publicly released and free to access.

B.1.6 Maintenance

Who is supporting/hosting/maintaining the dataset? The first author of this paper.

How can the owner/curator/manager of the dataset be contacted (e.g., email address)? The first author of this paper can be contacted via the email address given on the title page.

B.2. Relabeling e-SNLI-VE via MTurk

In this work, we collect new labels and explanations for the neutral pairs of the validation and test sets of e-SNLI-VE. We provide workers with the definitions of entailment, neutral, and contradiction for image-sentence pairs and one example for each label. As shown in Figure 7, for each

image-sentence pair, workers are required to (a) choose a label, (b) highlight words in the sentence that led to their label decision, and (c) explain their decision in a comprehensive and concise manner, using at least half of the words that they highlighted. We point out that it is likely that requiring an explanation at the same time as requiring a label has a positive effect on the correctness of the label, since having to justify in writing the picked label may make annotators pay an increased attention. Moreover, we implemented additional quality control measures for crowdsourced annotations, such as (a) collecting three annotations for every input, (b) injecting trusted annotations, and (c) restricting to annotators with at least 90% previous approval rate.

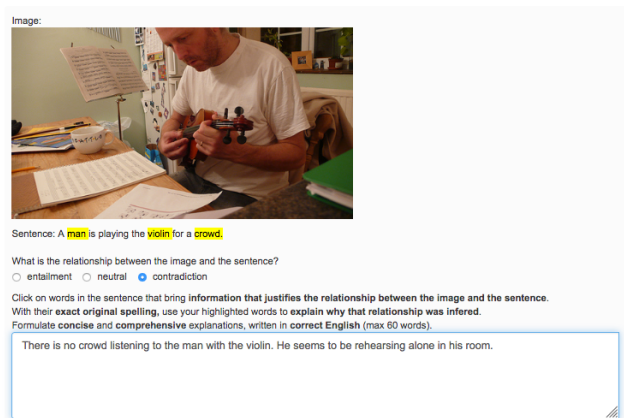


Figure 7: A snapshot of the annotation interface that was used to manually reannotate the neutral labels in the validation and test sets of e-SNLI-VE.

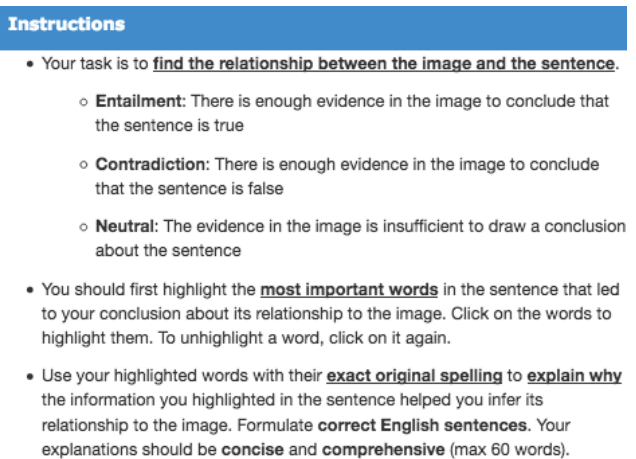


Figure 8: A snapshot of the instructions that were provided to the workers that reannotated the neutral labels in the validation and test sets of e-SNLI-VE.

There were 2,060 workers in the annotation effort, with an average of 1.98 assignments per worker and a standard deviation of 5.54. No restriction was put on the workers’ location. Each assignment consisted of a set of 10 image-sentence pairs. The instructions are shown in Figure 8. The annotators were also guided by three examples, one for each label. For each assignment of 10 questions, one trusted annotation with known label was inserted at a random position, as a measure to control the quality of label annotation. Each assignment was completed by three different workers.

To check the success of our crowdsourcing, we manually assessed the relevance of explanations among a random subset of 100 examples. A marking scale between 0 and 1 was used, assigning a score of k/n when k required attributes were given in an explanation out of n . We report an 83.5% relevance of explanations from workers.

B.3. Ambiguity in e-SNLI-VE

We noticed that some instances in SNLI-VE are ambiguous. We show some examples with justifications in Figures 10, 9, and 11. In order to have a better sense of this ambiguity, three authors of this paper independently annotated 100 random examples. All three authors agreed on 54% of the examples, exactly two authors agreed on 45%, and there was only one example on which all three authors disagreed. We identified the following three major sources of ambiguity: (1) mapping an emotion in the hypothesis to a facial expression in the image premise, e.g., “people enjoy talking”, “angry people”, “sad woman”. Even when the face is seen, it may be subjective to infer an emotion from a static image, (2) personal taste, e.g., “the sign is ugly”, and (3) lack of consensus on terms such as “many people” or “crowded”.

In our crowdsourced re-annotation effort, we accounted for this by removing an instance if all three annotator disagreed on the label (5.2% for validation and 5.5% test set). Otherwise we choose the majority label. Looking at the 18 instances where we disagreed with the label assigned by MTurk workers, we noticed that 12 were due to ambiguity in the examples, and 6 were due to workers’ errors.

B.4. Details on Filters

In Table 7, we provide a quantitative analysis of the effects our filters had on the dataset. The accuracies are obtained from our hand-annotated subset of 535 examples. On this subset, we first annotated every image-sentence pair as Entailment, Neutral, or Contradiction. Accuracies are obtained by comparing our own annotation with the dataset annotation. Note that we obtain higher error rates for the Entailment and Contradiction classes (9.7% and 8.6%) than what the authors of the original paper found [48] (less than 1%). One explanation for that could be the ambiguity that is inherent in the task. The share of bad explanations is obtained by evaluating every explanation as *bad*, *okay*, or

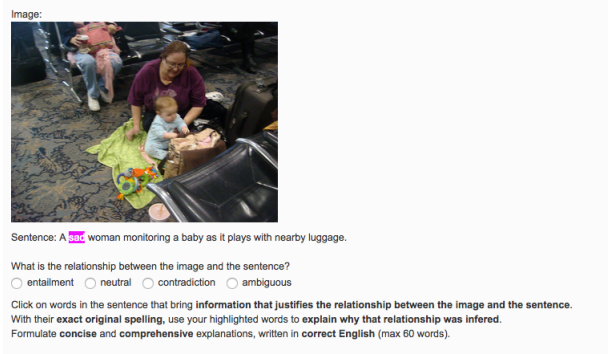


Figure 9: Ambiguous SNLI-VE instance. Some may argue that the woman’s face betrays sadness, but the image is not quite clear. Secondly, even with better resolution, facial expression may not be a strong enough evidence to support the hypothesis about the woman’s emotional state.

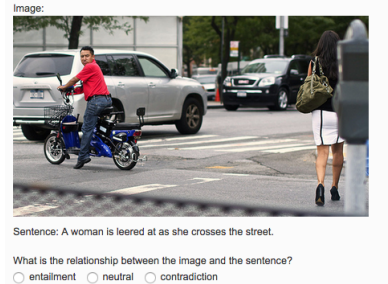


Figure 10: Ambiguous SNLI-VE instance. The lack of consensus is on whether the man is “leering” at the woman. While it is likely the case, this interpretation in favour of entailment is subjective, and a cautious annotator would prefer to label the instance as neutral.


Premise	Hypothesis	Label
	Kindergarten students napping	Neutral

Figure 11: Ambiguous SNLI-VE instance. Some may argue that it is impossible to certify from the image that the children are kindergarten students, and label the instance as neutral. On the other hand, the furniture may be considered as typical of kindergarten, which would be sufficient evidence for entailment.

great. If the label is wrong, the explanation is automatically deemed *bad*, as it will try to explain a wrong answer.

Note that in e-SNLI, the authors have found that the human annotated explanations have an error rate of 9.6%

(19.6% on entailment, 7.3% on neutral, 9.4% on contradiction), which serves as an upper bound of what could be achieved in terms of dataset cleaning.

An illustrative example for the motivation of the false neutral detector is given in the main paper in Figure 2. Examples for the keyword and similarity filters are given in Figures 12 and 13, respectively.



Textual premise: Older man sits and plays the accordion while young girl watches.
Hypothesis: An old man plays an instrument while a young child watches.
Label: Entailment
Explanation: An accordion is a type of instrument, also "child" is a synonym for "young girl" and "old man" is a rephrasing of "older man".

Figure 12: The use of the words “synonym” and “rephrasing” makes it clear that the explanation is overly focused on the linguistic features of the textual premise.



Textual Premise: A mother stands in a kitchen holding a small baby
Hypothesis: A mother is holding a small baby.
Label: Entailment
Explanation: A mother standing in the kitchen holding a small baby is the same as a mother holding a small baby.

Figure 13: The textual premise and hypothesis are almost identical sentences, which led to a low-quality explanation.

C. Benchmark Models

This section contains further details on the models that are compared in this benchmark.

C.1. Model Architectures

PJ-X. The PJ-X model [37] provides multimodal explanations for VQA tasks and was originally evaluated on VQA-X.

Its M_T module consists of a simplified MCB network [18] that was pre-trained on VQA v2.

We implemented PJ-X in PyTorch following closely the authors’ implementation in Caffe⁵. To address numerical optimization problems, we replaced the L2 normalization in the decoder with LayerNorm [7], as the original normalization zeroed gradients for earlier model parts. Additionally, we added gradient clipping of 0.1 to prevent too large gradients. To adapt PJ-X for multiple-choice question-answering in VCR, we follow the approach in the original VCR paper [50].

FME. The model introduced by Wu and Mooney [46], which we will refer to as FME (Faithful Multimodel Explanations), puts emphasis on producing faithful explanations. In particular, it aims to ensure that the explanation utilizes the same visual features that were used to produce the answer. Their code is not publicly available and we, therefore, re-implemented their base model according to the instructions in the paper. We chose the base model, as it was trained on the entire VQA-X 29.5K train split and the modifications of the other variations were difficult to re-implement from the descriptions in the paper. Our re-implementation of FME is based on a frozen modified UpDown [3] VQAv2 pre-trained VL-model.

Similarly to PJ-X, we also train FME with a gradient clipping of 0.1. To adapt FME for multiple-choice QA in VCR, we follow the approach in the original VCR paper [50].

RVT. The Rationale-VT Transformer (RVT) model [34] uses varying vision algorithms to extract information from an image and then feeds this information, the ground-truth answer, and the question to a pre-trained GPT-2 language model [38], which yields an explanation. As they omit the question answering part, we extend their model by an answer prediction module to allow for a fair comparison and to get a sense of the overall performance. We use their overall most effective visual input⁶, which are the tags of the objects detected in the image. As task model M_T , we use BERT [16], which takes as input the object tags and the question, and predicts the answer.

C.2. Joint or Separate Training.

All the VL-NLE models M in this work consist of M_T and M_E modules, which can either be trained jointly or separately. For the RVT model, training jointly would make no difference, as the explanation generation is not conditioned on a learnable representation in M_T (but instead on the fixed object tags for each image). For all other models,

⁵<https://github.com/Seth-Park/MultimodalExplanations>

⁶It obtained the highest visual plausibility score averaged across all datasets.

	Dataset Size			Share of wrong labels				Share of bad explanations			
	Train Set	Val Set	Test Set	All	E	N	C	All	E	N	C
Raw	529,505	17,554	17,899	19.3%	9.7%	38.6%	8.6%	35.7%	35.2%	45.1%	26.3%
FN removal	481,479	17,554	17,899	13.0%	9.7%	23.5%	8.6%	31.3%	35.2%	32.6%	26.3%
KW Filter	459,353	16,862	17,188	13.4%	10.1%	23.7%	8.8%	28.0%	28.3%	32.1%	24.6%
Uncertainty Filter	429,774	15,402	15,829	12.5%	10.1%	23.7%	4.5%	26.7%	28.3%	32.1%	19.5%
Similarity Filter	401,717	14,339	14,740	12.8%	10.5%	23.7%	4.5%	25.2%	24.1%	32.1%	19.5%

Table 7: Each row describes the state of the dataset upon application of the given filter. The share of wrong labels and bad explanations is only representative of the training split. The first row describes the state of the dataset in its raw form, i.e., before any of the automatic filtering steps. The second row describes the state of the datasets upon application of the false neutral (FN) removal filter, etc.

training jointly can be advantageous, because we backpropagate the explanation loss into the task model M_T , but this also comes at the risk of adverse effects on the optimization [14]. The authors of the PJ-X model mentioned that they tried both training approaches, but they do not specify which one worked best. Wu and Mooney [46] only trained separately. It should be noted that PJ-X and FME were both solely run on VQA-X, where a much larger dataset VQA v2 exists for task T . They pre-train M_T separately on this dataset, and it could be argued that, when training jointly, M_T runs the risk of becoming worse by overfitting on the smaller dataset VQA-X. For e-SNLI-VE and VCR, no such pre-training dataset exists. In this work, we train both jointly and separately for every model.

C.3. Reproducing Previous Results

In this work, we reproduced three different models. The code for RVT was publicly available and we only had to add a classifier that is suited for the input type of RVT. The code of PJ-X is also publicly available, albeit in an outdated version of the Caffe framework, and therefore we translated it into Pytorch. For FME no code is available and thus we re-implemented their model (as much as possible) according to the instructions given in the paper [46]. In Table 8 we show that the NLG metrics of our re-implementations come very close to those reported in the original papers.

For PJ-X and FME, we had to make a few minor deviations from the original implementations. To address issues with the gradients (vanishing and destabilizing) in PJ-X, we changed the L2 normalization to layer normalization [7] in the decoder, and added gradient clipping with a threshold of 0.1. FME was re-implemented in contact with the first author of the original paper. We re-implemented their “base” model, which leaves out some of their model extensions. This is motivated by the fact that these extensions either did not lead to performance increases for us (their \mathcal{L}_F loss) or are difficult to reproduce from the descriptions in the pa-

per (their dataset filter \mathcal{F}). For the sake of standardization, we use a ResNet-101 as feature extractor for both models. We also tried a ResNet-152, but this had little effect on our results.

C.4. Hyperparameters

In total, we have four models and three datasets. For PJ-X and FME, we choose the same hyperparameters as the authors across all datasets. For PJ-X, we also experimented with larger learning rates, as we experienced convergence issues. For RVT and e-UG, we conducted grid search on three batch sizes, three learning rates, and three ways to combine the loss. We compared dynamic weight loss [32] (with two loss temperatures $T = 2$ and $T = 0.5$) with simply adding both losses. However, this did not affect our results enough to warrant the increase in complexity. We selected the best configuration on VQA-X and then used these settings to train on e-SNLI-VE and VCR. For BERT on VCR, we had to use a higher batch size (128), as the results would not have converged otherwise. The final hyperparameters for all four models are reported in Table 9.

An additional overview of the differences between the models is given in Table 10.

C.5. Adaptations for VCR

To accommodate for the multiple-choice nature of task T , we adapt the architectures accordingly. For UNITER, we follow the original paper and formulate multiple-choice as a binary classification of question-image-answer tuples as True or False. The final answer is determined through a softmax of the four True scores. For PJ-X and FME, we follow the approach in the original VCR paper and obtain the logit for response j via the dot product of the final representation of the model and the final hidden state of the LSTM encoding of the response r^j [50]. For RVT, we use BERT-FORMULTIPLECHOICE from the transformers library [45].

Model		BLEU-4	METEOR	ROUGE-L	CIDEr	SPICE
PJ-X [37]	<i>Original</i>	19.8	18.6	44.0	73.4	15.4
	<i>Ours</i>	20.1	18.3	43.0	71.8	15.3
FME [46]	<i>Original</i>	23.5	19.0	46.2	81.2	17.2
	<i>Ours</i>	20.8	19.2	44.8	77.9	16.7

Table 8: A comparison (under the same settings) of automatic NLG metrics on VQA-X between our re-implementations (*Ours*) of PJ-X and FME and the results reported in the papers (*Original*).

	PJ-X	FME	RVT	e-UG
Batch Size	128	128	32* / 64	64
Learning Rate (LR)	7×10^{-4}	5×10^{-4}	5×10^{-5}	2×10^{-5}
Training Type	JOINT*	JOINT*	SEPARATE	JOINT
Loss Combination	$\mathcal{L}_T + \mathcal{L}_E$	$\mathcal{L}_T + \mathcal{L}_E$	N.A.	$\mathcal{L}_T + \mathcal{L}_E$
Optimizer	Adam	Adam	AdamW	AdamW for BERT
LR Scheduler	-	Step decay	Linear w/ warmup	Linear w/ warmup
Tokenization	Word	Word	WordPiece	WordPiece
Max Question Length	23	23	19	19
Max Answer Length	23	40	23	23
Max Explanation Length	40	40	51	51
Decoding	Greedy	Greedy	Greedy	Greedy

Table 9: Hyperparameters used for the different models across all datasets. \mathcal{L}_T and \mathcal{L}_E are the task loss and explanation loss, respectively. For RVT, the task batch size for VCR is 128, as 32 did not lead to convergence. For PJ-X and FME, we trained M_T and M_E separately on VQA-X.

Model	Vision	VL Model	Explanation Model	M_E Input
M	Backbone	M_T	M_E	
PJ-X	ResNet-101	MCB	LSTM (a)	image features, question, answer
FaiMu	ResNet-101	UpDown	LSTM (b)	image features, question, answer
RVT	Faster R-CNN	BERT	GPT-2	object tags, question, answer
e-UG	Faster R-CNN	UNITER	GPT-2	contextualized embeddings of image-question pair, question, answer

Table 10: Summary of the model differences.

D. Human Evaluation Framework

An example of the instructions that were shown to the MTurk annotators can be seen in Figure 14. The interface through which the annotators evaluated the explanations is displayed in Figure 15. The cost to evaluate *one* model on *one* dataset is 108-117\$.

E. Results

In this section, we present a benchmark evaluation with automatic NLG metrics (E.1), extended results on e-SNLI-

VE performance (E.2) and different ways to compute the e-ViL S_E score (E.4).

E.1. Automatic NLG Metrics

We report the automatic NLG scores in Table 11. Those are computed for all the explanations from the test sets where the predicted answer was correct. A quick observation is that the human evaluation results are not always reflected by the automatic metrics. For example, on the VCR dataset, FME, and not e-UG, obtains the highest S_E score when using automatic NLG metrics. Some tendencies are reflected nonetheless, such as the fact that e-UG is the best model

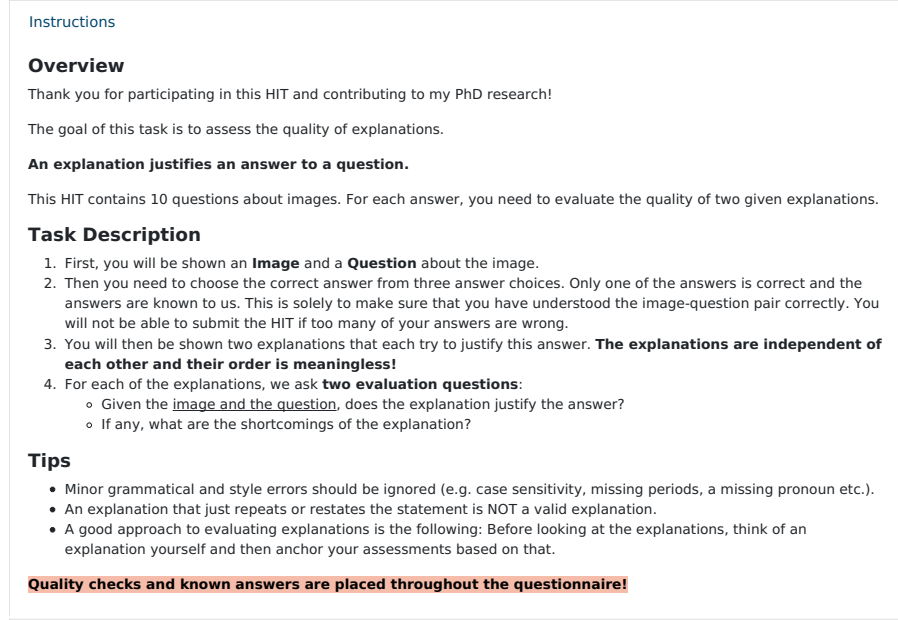


Figure 14: A snapshot of the instructions that were provided to the annotators that evaluated the explanations.

overall and that e-UG consistently outperforms RVT (albeit by a small margin).

Question-only GPT-2. In order to verify our intuition that the object labels used by RVT provide very little information about the image, we trained GPT-2 that only conditions on the question and answer, ignoring the image (called *GPT-2 only* in Table 11). Without having any image input, this model closely shadows the performance of RVT on most metrics. RVT is still slightly better in most cases, indicating that the object labels do provide some minor improvement. This suggests that RVT is not able to use visual information effectively and learns the explanations mostly based off spurious correlations and not based on the image.

E.2. Detailed Results for e-SNLI-VE

Here, we provide more detailed results on our newly released e-SNLI-VE dataset. We break down the task accuracy and explanation scores by the three different classes (see Table 12). For all models, we observe significantly lower accuracies and explanation scores for the neutral class. There are two potential explanations for this. First, the neutral class can be harder to identify than the other classes. In image-hypothesis pairs, entailment and contradiction examples can sometimes be reduced to more straightforward yes/no classifications of image descriptions. For the neutral class, there always needs to be some reasoning involved to decide whether the image does (not) contain enough evidence to neither indicate entailment nor contradiction. A second reason is that, despite our best efforts to clean the dataset, the neutral class is still more noisy and less represented in the training data.

E.3. Statistical Analysis of the S_E Score

To ensure high quality of our results, we had a number of in-browser checks that prevented the annotators from submitting the questionnaire when their evaluations seemed of poor quality. Checks include making sure that they cannot simultaneously say that an explanation is insufficient (they select the *No* or *Weak No* option described in Section 4) and has no shortcomings, or that it is optimal (they select *Yes* option), but has shortcomings. We also experimented with further post-hoc cleaning measures (such as verifying that they evaluated the ground-truth favorably or did not always choose similar answers), but they had a negligible impact and thus were disregarded.

Our MTurk sample consists of 19,194 evaluations, half of which are for ground-truth explanations, and the other half for model generated explanations. We obtain evaluations for 264 to 299 unique question-image pairs for every model-dataset combination, leaving us with explanations missing for only 3.3% of questions. There are 82.1 evaluations per annotator on average ($SD = 170.1$), ranging from 16 to 1,244 with a median of 34. After pooling annotations of the same explanation, 6,494 annotations remain (887 to 897 for the evaluations generated by each model).

In Figure 16, we add standard errors to the numerical S_E scores given in Table 3. This figure confirms that e-UG uniformly outperforms the other models.

To further investigate the robustness of the e-ViL benchmark, we do a statistical analysis of our S_E scores by using a Linear Mixed Model (LMM) that predicts S_E from the

<i>VQA-X</i>	e-ViL Scores (auto)			<i>n</i> -gram Scores								Learned Sc
	S_O	S_T	S_E	B1	B2	B3	B4	R-L	MET.	CIDEr	SPICE	BERTScore
PJ-X [37]	32.1	76.4	42.1	57.4	42.4	30.9	22.7	46.0	19.7	82.7	17.1	84.6
FME [46]	33.0	75.5	43.7	59.1	43.4	31.7	23.1	47.1	20.4	87.0	18.4	85.2
RVT [34]	26.8	68.6	39.1	51.9	37.0	25.6	17.4	42.1	19.2	52.5	15.8	85.7
GPT-2 only	N.A.	N.A.	37.8	51.0	36.4	25.3	17.3	41.9	18.6	49.9	14.9	85.3
e-UG	36.5	80.5	45.4	57.3	42.7	31.4	23.2	45.7	22.1	74.1	20.1	87.0
<i>VCR</i>												
PJ-X [37]	7.2	39.0	18.4	21.8	11.0	5.9	3.4	20.5	16.4	19.0	4.5	78.4
FME [46]	17.0	48.9	34.8	23.0	12.5	7.2	4.4	22.7	17.3	27.7	24.2	79.4
RVT [34]	15.5	59.0	26.3	18.0	10.2	6.0	3.8	21.9	11.2	30.1	11.7	78.9
GPT-2 only	N.A.	N.A.	26.3	18.0	10.2	6.0	3.8	22.0	11.2	30.6	11.6	78.9
e-UG	19.3	69.8	27.6	20.7	11.6	6.9	4.3	22.5	11.8	32.7	12.6	79.0
<i>e-SNLI-VE</i>												
PJ-X [37]	26.5	69.2	38.4	29.4	18.0	11.3	7.3	28.6	14.7	72.5	24.3	79.1
FME [46]	29.9	73.7	40.6	30.6	19.2	12.4	8.2	29.9	15.6	83.6	26.8	79.7
RVT [34]	31.7	72.0	44.0	29.9	19.8	13.6	9.6	27.3	18.8	81.7	32.5	81.1
GPT-2 only	N.A.	N.A.	43.6	29.8	19.7	13.5	9.5	27.0	18.7	80.4	32.1	81.1
e-UG	36.0	79.5	45.3	30.1	19.9	13.7	9.6	27.8	19.6	85.9	34.5	81.7

Table 11: Automatic NLG metrics for all model-dataset pairs. The S_E based on automatic NLG metrics is the harmonic mean that was used to select the best model during validation. B1 to B4 stand for BLEU-1 to BLEU-4, R-L for ROUGE-L, and MET for METEOR.

	Entailment			Neutral			Contradiction		
	Acc.	MET.	BERTS.	Acc.	MET.	BERTS.	Acc.	MET.	BERTS.
PJ-X	74.4	14.0	79.2	61.5	12.4	77.4	72.8	15.9	79.3
FME	77.3	15.1	79.8	67.3	13.5	77.9	77.2	16.3	79.8
RVT	74.6	17.9	81.3	63.3	19.0	80.7	79.4	19.4	81.4
e-UG	80.3	19.6	81.6	71.7	18.5	80.9	87.5	20.9	82.6

Table 12: Class-wise results on e-SNLI-VE for the different models. NLG metrics are only shown for METEOR and BERTScore, as those correlate most with human judgement.

model-dataset pairs, with model as fixed factor and dataset as random effect. LMM predicts the evaluations with the Likelihood-Ratio-Test of the fixed effect being significant, with $\chi^2(3) = 37.462, p < 0.001$. To gain better insight, we performed post-hoc pairwise contrasts, which indicate that e-UG significantly outperforms the remaining models, with $p < 0.001$. Further, RVT outperforms PJ-X significantly, with $p = 0.007$. The significance level was adjusted for a family-wise type I error rate of $\alpha = 0.05$ using Bonferroni-Holm adjustments.

E.4. Alternative S_E Scores

The nature of our human evaluation questionnaire allows for multiple ways to compute the e-ViL score S_E of the generated explanations. The key differences between the scoring methods are on how to pool the up-to-three evaluations we have for each explanation, and how to compute the overall numerical value. In the main paper, we compute S_E by mapping the four evaluation choices to numerical values, then taking the average for every explanation in the sample and then the sample average to get our S_E score. Below, we propose two alternative ways to compute S_E . While they

Image:



Question: What is the person doing?

What is the correct answer to the question?

☐ main

☐ ivory

☐ snowboarding

Explanation #1: He leans his body forward to glide down the mountain.

a) Given the above image and question, does this explanation justify the answer to the question?

☐ Yes

☐ Weak Yes

☐ Weak No

☐ No

b) What are the shortcomings of the explanation?

☐ Incorrect description of the image

☐ Insufficient justification

☐ Confusing sentence

☐ None

Figure 15: A snapshot of the interface through which annotators evaluated the explanations.

lead to different values, the performance differences between our models remain relatively similar.

E.4.1 Median Pooling

In median pooling, we obtain the score for each explanation by taking the median of its up-to-three ordinal evaluations (as opposed to taking a numerical average). We always interpolate with rounding off, meaning that the median of (*Yes*, *Weak Yes*) \mapsto *Weak Yes* and (*Yes*, *No*) \mapsto *Weak No*. This allows us to plot the distribution of *No*, *Weak No*, *Weak Yes*, and *Yes* for every model-dataset pair, as displayed in Figure 18.

We observe that e-UG performs better across all datasets, with RVT following in second place for the VCR and VQA-

X datasets. The differences between the PJ-X, FME and RVT are relatively small.

We analyse our results using a Cumulative Link Mixed Model (CLMM) with a logit link and flexible thresholding. We predict annotator responses using the dataset as random effect and the VL-NLE model as fixed effect. We find that the model significantly influences ratings, as suggested by the Likelihood-Ratio-Test, $\chi^2(2) = 42.4, p < 0.001$, when comparing the full model to a nested statistical model that is merely based on the dataset as predictor. The model predictor is dummy-coded with e-UG as reference class, which enables us to interpret the model’s coefficients in the statistical test as pairwise contrasts of all other models towards e-UG. All coefficients have p -values $p < 0.001$, indicating the e-UG significantly outperforms all other models.

E.4.2 Comparative S_E Score

We also designed a comparative score, for which we do not map our questionnaire evaluation options (*No*, *Weak No*, *Weak Yes*, and *Yes*) to numerical values, but instead compare them to the evaluation of the ground-truth. For every image-question pair, the annotator has to evaluate both the ground-truth and the generated explanation, without knowing which is which. This enables us to see, for every generated explanation, if it was deemed equally good, better, or worse than the ground-truth. This mimics the approach in Park et al. [37] and Wu and Mooney [46], where annotators were explicitly asked if the generated explanation was worse, equally good, or better than the ground-truth. An advantage of this method is that we can seamlessly incorporate the criticalness of each annotator. The disadvantage is that we do not get *absolute* measurements of the quality of the explanations.

The generated explanation gets the score 1 if it is as good or better than the ground-truth, and otherwise 0. We pool the comparative score via median pooling with rounding off.

Figure 17 displays the comparative score. We can observe that e-UG scores are strongest across all datasets, while the other three models are performing similarly, except on the VCR dataset, where PJ-X performs worse than the other models.

For our statistical analysis, we fit a generalized linear mixed model (GLMM) on the full unpooled annotation set predicting the whether an explanation was rated positively (compared to the ground-truth) using the dataset and annotator as random effects and the VL-NLE model as fixed effect. We utilise a logit link. The model parameter significantly predicts the evaluations, with $\chi^2(3) = 67.366, p < 0.001$. Post-hoc tests (Tukey contrasts with Bonferroni-Holm adjusted significance) show that the e-UG outperforms all other models, with $p < 0.001$, and that RVT outperforming PJ-X at $p = 0.011$. All other pairwise comparisons were not significant. Extending the model to include ground-truth

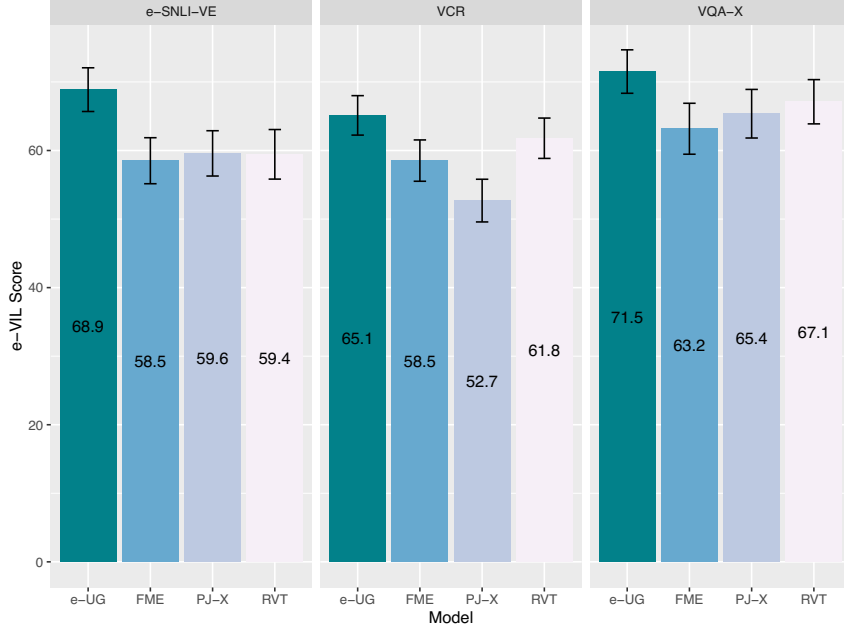


Figure 16: Human evaluation framework: e-ViL scores S_E . This plot shows the main e-ViL scores (based on numerical average) for the different model-dataset pairs. Error bars show $\pm 2SD/\sqrt{n}$ for each group.

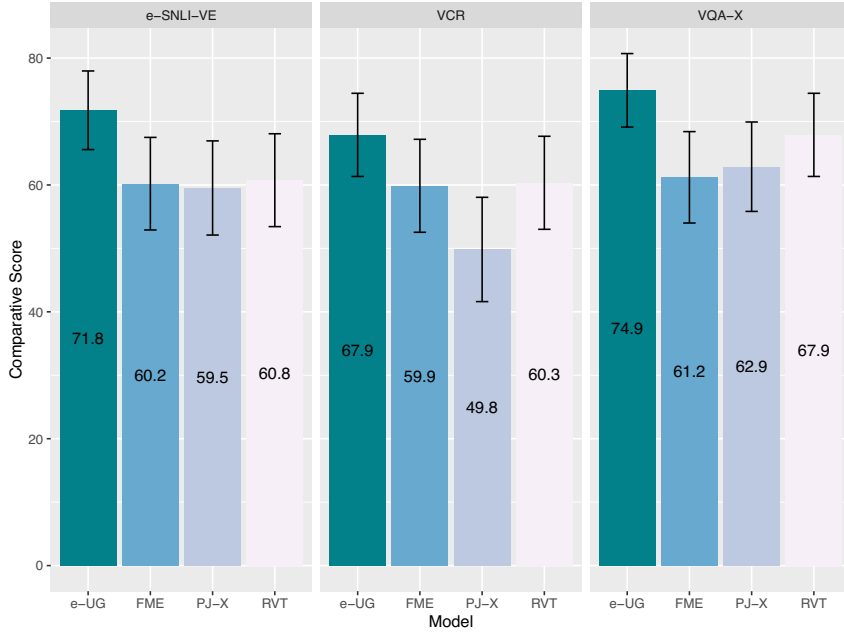


Figure 17: Human evaluation framework: Comparative scores. This figure displays the comparative scores (with respect to the ground-truth) of the explanations for the different model-dataset pairs. Error bars show $\pm 2SD/\sqrt{n}$ for each group.

explanations as a model category also demonstrates that all model-generated explanations were evaluated significantly worse than the ground-truth explanations. We conclude that the e-UG outperforms all other models, whereas perfor-

mance differences between them are rather small, replicating our findings from the alternative analyses.

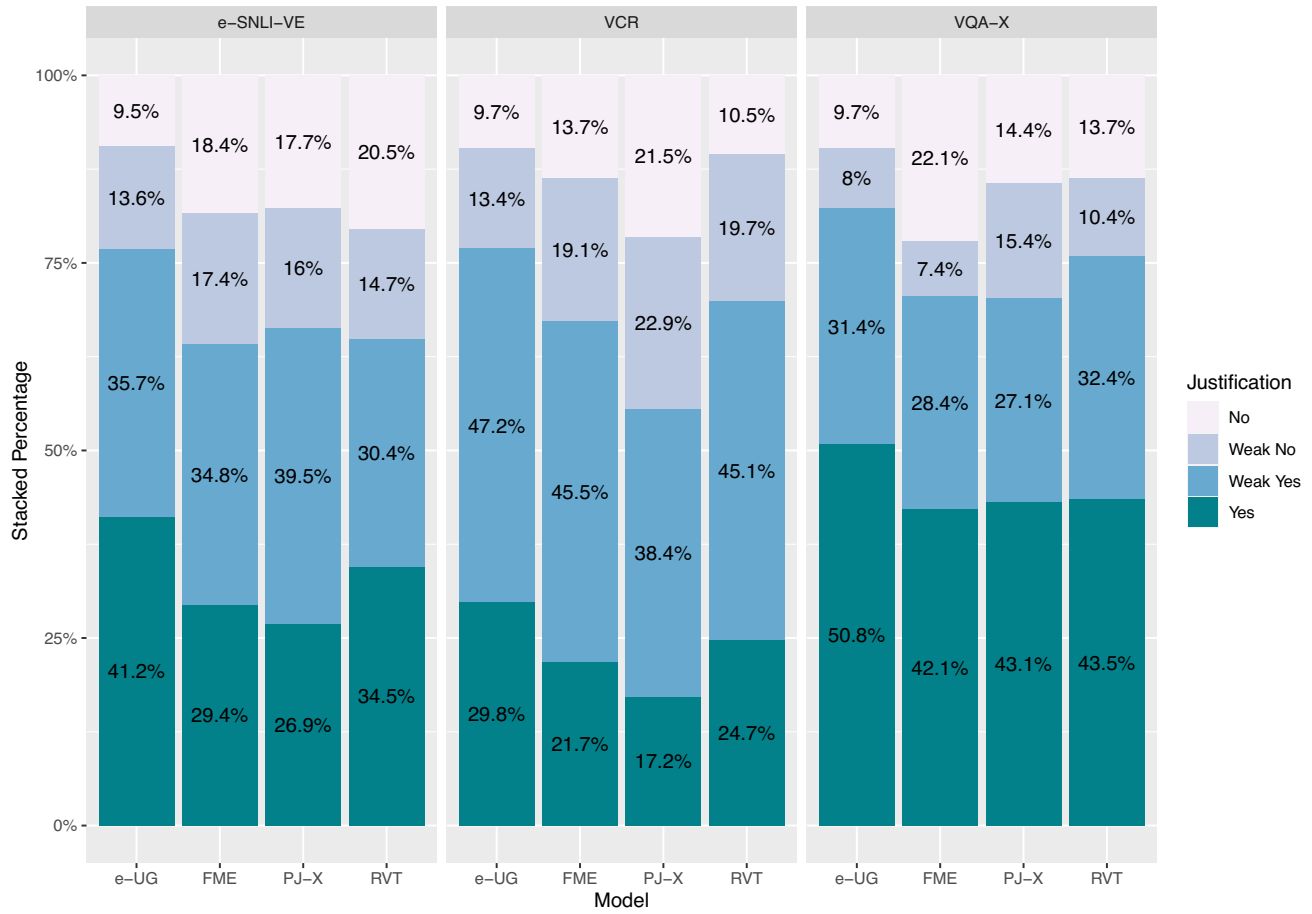


Figure 18: Human evaluation framework: Ordinal representation of the evaluations. Median responses for each question-image pair given by participants to the evaluation question “Given the image and the question/hypothesis, does the explanation justify the answer?”.